J. Hydrol. Hydromech., 64, 2016, 2, 196–208
DOI: 10.1515/johh-2016-0016

Root distributions in a laboratory box evaluated using two different techniques (gravimetric and image processing) and their impact on root water uptake simulated with HYDRUS

Aleš Klement*, Miroslav Fér, Šárka Novotná, Antonín Nikodem, Radka Kodešová

Department of Soil Science and Soil Protection, Faculty of Agrobiology Food and Natural Resources, Czech University of Life Sciences Prague, Kamýcká 129, 165 21 Prague 6, Czech Republic.
* Corresponding author. Tel.: +420 224 382 757. E-mail: klement@af.czu.cz

Abstract: Knowledge of the distribution of plant roots in a soil profile (i.e. root density) is needed when simulating root water uptake from soil. Therefore, this study focused on evaluating barley and wheat root densities in a sand-vermiculite substrate. Barley and wheat were planted in a flat laboratory box under greenhouse conditions. The box was always divided into two parts, where a single plant row and rows cross section (respectively) was simulated. Roots were excavated at the end of the experiment and root densities were assessed using root zone image processing and by weighing. For this purpose, the entire area (width of 40 and height of 50 cm) of each scenario was divided into 80 segments (area of 5x5 cm). Root density in each segment was expressed as a root percentage of the entire root cluster. Vertical root distributions (i.e. root density with respect to depth) were also calculated as a sum of root densities in each 5 cm layer. Resulting vertical root densities, measured evaporation from the water table (used as the potential root water uptake), and the Feddes stress response function model were used for simulating substrate water regime and actual root water uptake for all scenarios using HYDRUS-1D. All scenarios were also simulated using HYDRUS-2D. One scenario (areal root density of barley sown in a single row, obtained using image analysis) is presented in this paper (because most scenarios showed root water uptakes similar to results of 1D scenarios).

The application of two root detecting techniques resulted in noticeably different root density distributions. Differences were mainly attributed to the fact that fine roots of high density (located mostly at the deeper part of the box) had lower weights in comparison to the weight of few large roots (at the box top). Thus, at the deeper part, higher root density (with respect to the entire root zone) was obtained using the image analysis in comparison to that from the gravimetric analysis. Conversely, lower root density was obtained using the image analysis at the upper part in comparison to that from the gravimetric analysis. On the other hand, fine roots overlapped each other and therefore were not visible in the image, which resulted in lower root density values from image analysis. Root water uptakes simulated with HYDRUS-1D using diverse root densities obtained for each cereal declined differently from the potential root water uptake values depending on water scarcity at depths of higher root density. Usually, an earlier downtrend associated with gradual root water uptake decreases and vice versa. Similar root water uptakes were simulated for the presented scenario using the HYDRUS-1D and HYDRUS-2D models. The impact of the horizontal root density distribution on root water uptake was, in this case, less important than the impact of the vertical root distribution resulting from different techniques and sowing scenarios.

Keywords: Flat laboratory box; Image analysis; Gravimetric analysis; Root distribution; Root water uptake; Mathematical modeling.

INTRODUCTION

Plant roots considerably affect water regimes in soil profiles due to plant transpiration (e.g. Novák, 2012). They also affect soil structure and may cause a preferential water flow and transport of contaminants (e.g. Kodešová et al., 2006, 2015). Diversity in root architecture associates with a plant water efficiency (Tron et al., 2015). The architecture of plant roots (root distribution, length, diameter, strength etc.) depends on the plant species and its interaction with soil conditions (Bengough et al., 2011; Hallett et al., 2013; Loades et al., 2013; Nikodem et al., 2013). Root distribution can be studied directly in the field or in differently designed laboratory boxes using various techniques (Maeght et al., 2013; Neumann et al., 2009). Field root development analysis can be performed using non-destructive methods, i.e. using minirhizotron digital cameras or scanners (Iversen et al., 2012; Shilo et al., 2013). Root distribution may be also studied using destructive techniques, such as 3D roots system excavation, root sampling and root system imaging in vertical field sections (trenches), soil coring, etc. (Maeght et al., 2013).

The growth of roots and their architecture is becoming increasingly studied in the laboratory using specially designed flat boxes and under hydroponic conditions or in variable soil substrates. Depending on the conditions used and box design (i.e. thickness, transparency etc.), roots can be either directly photographed or the neutron, x-ray computed tomography, NMR, 2D light transition imaging technique can be applied (de Dorlodot et al., 2007; Doussan et al., 2006; Garrigues et al., 2006; Moradi et al., 2009, 2010, 2013; Moran et al., 2000; Oswald et al., 2008; Rudolph et al., 2012, 2013; Rudolph-Mohr et al., 2014; Stingaciu et al., 2013). These techniques were mostly applied to analyze root development in the early stage of plant and roots growth. Data have been used to validate root growth mathematical models and root water extraction models (e.g. Doussan et al., 2006; Stingaciu et al., 2013).

A more robust approach must be applied for expressing the root system when simulating the crop (cereals, maize etc.) root

water uptake using many available mathematical models (e.g. HYDRUS Software Packages, Šimůnek et al., 2008), which describe the interaction between soil, plant and atmosphere. For this purpose a root system is usually characterized by a root density distribution within the soil profile, which must be evaluated beyond the early stage of root growth. In this case, field studies are more appropriate, or root growth in the laboratory boxes should be designed to last a longer time. A possible method for detailed root density analysis is a gravimetric analysis of roots extracted from soil blocks that have been sampled from the soil profile (e.g. Himmelbauer and Novák, 2008; Himmelbauer et al., 2010, 2013; Zhang et al., 2015). Himmelbauer and Novák (2008) and Himmelbauer et al. (2004, 2013) also scanned root fragments and applied an image analysis to characterize root length, diameter classes and surface areas. To our knowledge, there is no study, which attempts to scan the entire root system and to determine root density from these images only, as well as any study that compares root densities obtained using these two methods (i.e. gravimetric and image analysis). We also did not find any study, which uses such information for mathematical modeling of root water uptake and evaluates the impact of root densities obtained using different techniques on simulated data. Nor does there exists any study, which analyzes the difference between root water uptakes simulated using root distributions characterized within the 1D or 2D soil profiles. Therefore, the goal of this study was to assess the fitness of two methods for describing the root distribution of two cereals (barley and wheat). Another goal was to assess how the root densities obtained using different techniques influence root water uptake simulated using HYDRUS-1D and 2D codes.

MATERIAL AND METHODS

Laboratory box experiment

The study was performed under greenhouse conditions in a flat box (length of 100, thickness of 3, and height of 60 cm). Thickness of the box was designed to reduce wall restriction at the early stage of root growth. The box consisted of a metallic frame with a perforated bottom and opened top. Large vertical sides made of Plexiglas panels allowed for root growth observation. The bottom of the box was covered with a highly permeable textile, on which a 5 cm drainage layer was formed using coarse technical quartz sand (ST10/40 - particle size 1 mm, from the sand mine Sklopísek Střeleč). This was again covered with a highly permeable textile. A drainage layer and perforated bottom allowed for fast discharge of redundant gravitational water from the box. Discharge water was collected, but this information was not recorded during our study. Next, a substrate consisting of fine technical quartz sand (ST08 - particle size of 0.10–0.63 mm, from the same sand mine) and vermiculite (particle size of 1 mm) in the ratio 15:1 was packed in the box (layer thickness of 50 cm). Such substrate was selected to reduce the impact of mechanical impedance and water stress restricting root growth (Bengough et al., 2011), and to allow for relatively easy roots excavation. The box sides were covered by isolating layers of aluminum foil and geotextile to prevent direct sunlight and reduce heat transfer towards the root zone.

Two cereals, barley (*Hordeum vulgare* L.) and wheat (*Triticum aestivum* L.), were subsequently planted in this box. The box was always divided into two parts, which were not separated by any construction. In one half, seeds were sown in one row 40 cm long (approximately 70 seeds) (A) and in the second half, in 4 spots (approximately 5 seeds of barley per spot, spot distance of 10 cm) or 3 spots (approximately 7 seeds of wheat per spot, spot distance of 15 cm), which simulated a planting rows cross section (B). During both experiments, the temperature varied between 20 – 27°C. Due to its low water retention capacity, the substrate was watered twice a week using 2 liters of water (rate of 6.67 cm min^{-1}) with fertilizer (ratio of nitrogen : phosphorus (P_2O_5) : potassium (K_2O) (7 : 3 : 6%)) (compound concentration was 700 mg l^{-1} of nitrogen, 65 mg l^{-1} of phosphorus, and 498 mg l^{-1} of potassium). The first experiment lasted 90 days and the second experiment 114 days. Experiments were always terminated when plants started to die back, i.e. at the shooting stage of barley and heading stage of wheat. Next, the box was turn on its side and one Plexiglas panel was unmounted. Substrate was air dried for several days and then carefully removed using a brush. The extracted roots (separately for plant row and plant rows cross section) were placed on a square mesh (5x5 cm). Root transfer was done very carefully to keep a natural 2D composition of roots within the vertical flat box area, which was in all cases the same (width of 40 and height of 50 cm) (Figure 1). The entire root systems were photographed using a NIKON D700 camera with a resolution of 12.1 Megapixels, and fitted with a NIKON 24-85 mm zoom lens with a minimum aperture of F2.8-4. Each root system was photographed only from one side because it was not possible to turn roots without any changes in their position within the mesh. Images were taken at a resolution of 200 dpi. The size of the image was 4 096 × 3 072 pixels; the size of the pixel side was 13.8 μm. Roots were then cut along the mesh network into 80 root segments, cleaned with water, dried and weighed.

Two methods were used to evaluate root density. First, the images of roots were analyzed using ImageJ software version 1.47 (Rasband, 1997–2014) (I). The function Color threshold, which allows the selecting of pixels of a particular color range, was used to detect roots. Next, the image was divided into 80 separate segments (area of 5x5 cm) and the area of roots covering each segment was evaluated using IsoData algorithm function. The root density in each segment (*RDS*) (i.e. areal root density within 2D soil profile) was then expressed in percentages as follows:

$$RDS(x,z) = \frac{A(x,z)}{\sum_{z=1}^{M}\sum_{x=1}^{N} A(x,z)} 100 \quad (1)$$

where A(x, z) is the root area in the particular segment, x and z are horizontal and vertical axes of the segment center, and N and M are number of segments in horizontal and vertical direction, respectively. The root density with respect to depth (*RDD*) (i.e. vertical root density within the 1D soil profile) was also calculated:

$$RDD(z) = \sum_{x=1}^{N} RDS(x,z) \quad (2)$$

Second, the root density was calculated using the root masses (G). The same equations (1) and (2) were used, except that in this case, A(x, z) was the root mass in the particular segment.

Statistical analysis

The average, standard deviation, coefficient of variation, minimum and maximum was calculated for each set of evaluated root densities (i.e. using areal root densities from all combinations A/I, A/G, B/I and B/G for barley and wheat, respectively,

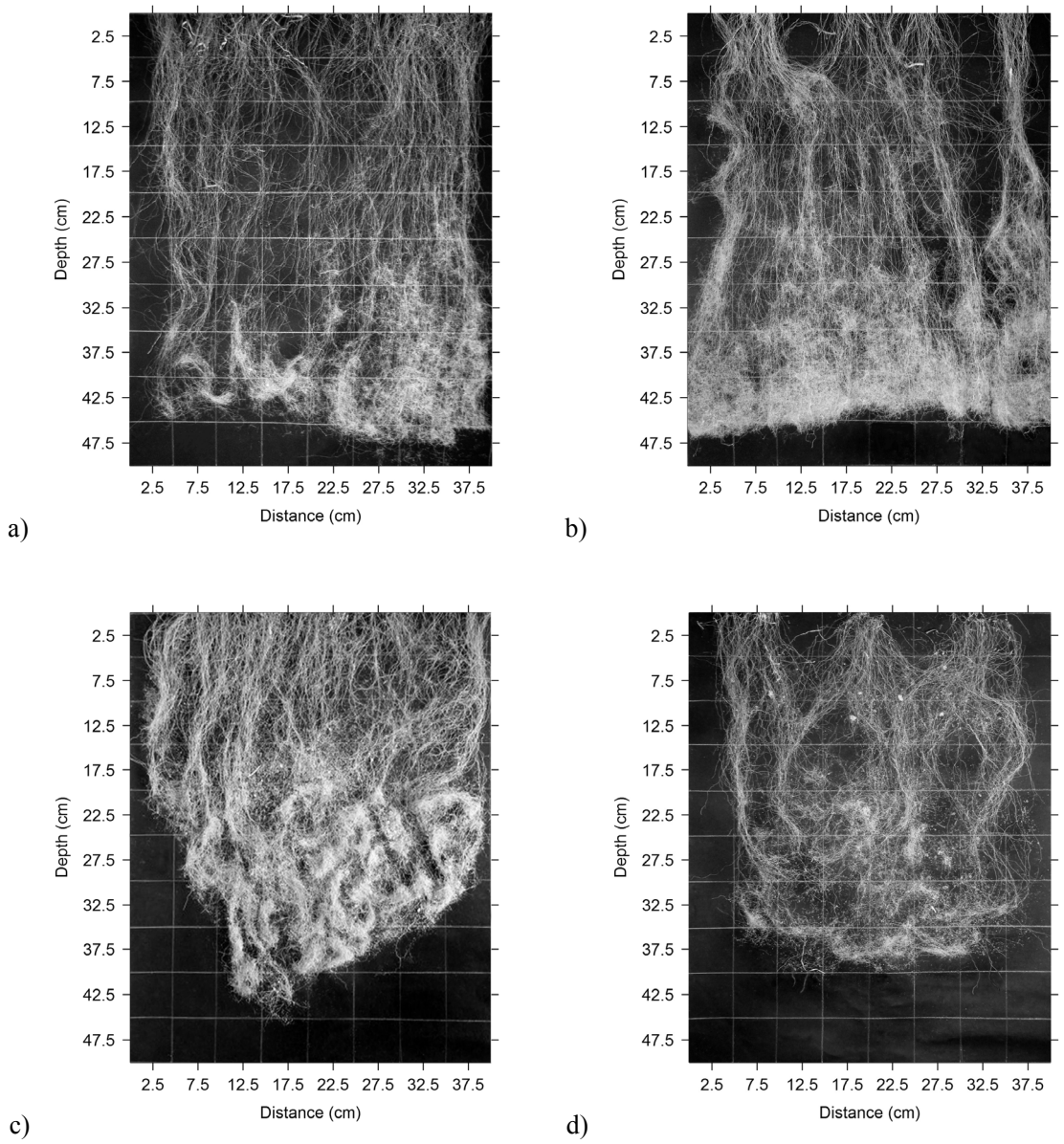

Fig. 1. Photos of roots of barley sown in single row (a) and 4 spots (b) and of wheat sown in single row (c) and 3 spots (d).

and also all vertical root densities). The relationships between areal root densities obtained using two different techniques (I or G) for a particular cereal and plant arrangement (i.e. A/I and A/G, B/I and B/G for barley and wheat, respectively) were assessed using the Pearson correlation coefficient and p-value (i.e. multiple variable analysis was performed using Statgraphics, 2009). The Pearson correlation coefficients and p-values were also calculated to evaluate relationships between vertical root densities obtained from different techniques (I or G) and also from different plant arrangements (A or B). Analyses were performed using all values in a 2D (80 square segments) or 1D (10 layers) soil profile. Since some layers did not contain any roots, or the evaluated values were negligible, zero and very low values (root densities *RDS* and *RDD* below 0.05 and 2, respectively) were removed from all datasets and analyses were repeated. P-values below 0.05 indicate statistically significant non-zero correlations at the 95.0% confidence level. The statistical significances at the 99.0 and 99.9% confidence levels were also distinguished.

Mathematical modeling of root water uptake

The resulting root densities were used as inputs into the mathematical models simulating water regime in soils to assess the impact of different root densities on a simulated root water uptake. The theoretical example was designed to focus solely on the simulated root water uptake: 1. The same initial conditions were applied for all scenarios, which were set at low pressure head values to quickly achieve the pressure heads of decreased water availability for plants; 2. No water irrigation at the top was assumed; 3. No simulated flux at the bottom was expected (i.e. setting initial conditions at low pressure head values did not allow water discharge from the box); 4. The same potential transpiration was used in all cases.

First, the influence of the different root densities within the 1D profile (obtained for two cereals, two sowings and using two detection techniques) on the root water uptakes from the laboratory substrate was studied. Water regime in substrate and root water uptake was simulated using the HYDRUS-1D pro-

gram (Šimůnek et al., 2008). The Richards equation, describing the one-dimensional isothermal Darcian flow in a variably saturated rigid porous medium, is used in the model:

$$\frac{\partial \theta}{\partial t} = \frac{\partial}{\partial z}\left(K(h)\frac{\partial h}{\partial z} + K(h) \right) + S \tag{3}$$

where θ is the soil water content [L^3L^{-3}], h is the pressure head [L], K is the hydraulic conductivity [LT^{-1}], S is the sink term [T^{-1}] (i.e. root water uptake), t is time [T], and z is the vertical axis [L]. The van Genuchten (1980) analytical expressions are used to describe soil hydraulic functions, the soil water retention curve, θ(h), and the hydraulic conductivity function, $K(\theta)$:

$$\theta_e = \frac{\theta(h) - \theta_r}{\theta_s - \theta_r} = \frac{1}{\left(1 + |\alpha h|^n\right)^m} \quad h < 0 \tag{4}$$

$$\theta_e = \theta_s \quad h \geq 0$$

$$K(\theta) = K_s\ \theta_e^l \left[1 - (1 - \theta_e^{1/m})^m\right]^2 \quad h < 0 \tag{5}$$

$$K(\theta) = K_s \quad h \geq 0$$

where θ_e is the effective soil water content [dimensionless], K_s is the saturated hydraulic conductivity [LT^{-1}], θ_r and θ_s are the residual and saturated soil water contents [L^3L^{-3}], respectively, l is the pore-connectivity parameter [dimensionless] (l = 0.5), α is reciprocal of the air entry pressure, [L^{-1}], and n [dimensionless] is related to the slope of the retention curve at the inflection point, and $m = 1 - 1/n$ [–].

The root water uptake in (3) is calculated assuming the Eq. 6 proposed by Feddes et al. (1978).

$$S(z,t) = \alpha_R(h)\, b(z)\, T_P(t) \tag{6}$$

where T_p [LT^{-1}] is the potential plant transpiration, $\alpha_R(h)$ [−] is the alpha-function characterizing the plants ability to extract water from soil, which depends on the pressure head, and b(z) [L^{-1}] is the normalized water uptake distribution, which is evaluated from any arbitrarily measured or prescribed root distribution function b'(z).

$$b(z) = \frac{b'(z)}{\int_{L_R} b'(z)dz} \text{ thus } \int_{L_R} b(z)\,dz = 1 \tag{7}$$

where L_R [L] is the region occupied by the root zone.

The depth of simulated vertical flow domain was 55 cm, which was divided into layers: 50 cm of substrate and 5 cm of drainage layer. The parameters of the soil hydraulic functions (4) and (5) were measured in the laboratory on 100-cm^3 soil samples (soil core height of 5.1 cm and cross-sectional area of 19.60 cm^2) placed in Tempe cells using the multistep outflow experiment (van Dam et al., 1994) and constant head test (Dane and Topp, 2002) (Table 1). Initial conditions were set as hydrostatically distributed pressure heads with a pressure head of –100 cm at the bottom and –155 cm at the top (i.e. steady state at the sand water holding capacity). The atmospheric boundary condition with no precipitation and evaporation (surface was mostly covered by plants) was set at the top, and seepage face at the bottom. Root water uptake was simulated assuming an evaluated root zone depth and density (i.e. 4 scenarios, corresponding to two sowings and two methods of root density analysis, were simulated for each cereal), the Feddes stress response function model [6] with parameters for wheat (h_1 = 0, h_2 = –1, h_3 = –500 and –900 cm for potential transpiration equal to 0.5 and 0.1 cm day^{-1}, respectively, and h_4 = –16000 cm), and hourly potential transpiration rates. The potential transpiration was set as water evaporation from the shallow pan (diameter of 19.7 cm) placed on balances, which was monitored during the experiments. For comparison of root water uptakes of two cereals (which had different root depths and densities) we used a 60 hour period obtained at the end of the first experiment (i.e. 60 hours prior to disassembling the experiment). The data are shown together with the simulated actual transpirations (root water uptakes) in the results section. The uncompensated root water uptake was considered, i.e. the critical stress index in root water uptake model was equal to one.

Next the difference between the root water uptake calculated using the 1D model (i.e. using only vertical root density within the 1D soil profile) and that calculated using the 2D model (i.e. using areal root density within the 2D soil profile) was evaluated. Only one scenario (for root distribution of barley in the row obtained using image analysis, i.e. barley A/I) simulated using HYDRUS-2D is presented here as an example (since we did not observe significant differences between root water uptakes from all corresponding 1D and 2D scenarios). Flow domain was designed as a vertical plane (height of 55 cm and width of 40 cm). The soil hydraulic properties, initial and boundary (top and bottom) conditions were set similarly to the 1D scenario. Zero water flux was assumed at the vertical boundaries (to obtain comparable results with the 1D simulation). Root densities were set according to the areal root densities, evaluated using the image analysis. The resulting root water uptake, which describes the water discharge from the entire 2D flow domain due to plant transpiration was divided by the length of the top boundary (40 cm) for comparison with the root water uptake representing water discharge from the 1D flow domain due to plant transpiration (i.e. results simulated with HYDRUS-1D). It should again be pointed out that zero discharge from the bottom flow domain was simulated in all cases (i.e. all 1D and 2D scenarios), because initial conditions were set at sand water holding capacity at the bottom and no water was added into the flow domain during the simulations.

Table 1. Van Genuchten soil hydraulic parameters θ_r, θ_s, α, n and K_s.

Material	Layer thickness (cm)	θ_r (cm^3cm^{-3})	θ_s (cm^3cm^{-3})	α (cm^{-1})	n –	K_s (cm $hour^{-1}$)
Fine sand and vermiculite	50	0.022	0.416	0.053	3	15.3
Coarse sand	5	0.010	0.400	0.190	3	750

RESULTS AND DISCUSSION

Comparison of root distributions obtained using two different techniques

Figure 1 shows photos of extracted roots from the substrate. The resulting areal root densities for barley and wheat are shown in Figures 2 and 3, respectively. Vertical root densities are shown in Figure 4. Figure 5 shows the relationship between vertical root densities evaluated using both techniques. Figures 1–5 show noticeably different root densities and patterns obtained using both techniques. It should be pointed out that the evaluated root densities are always related to the entire root zone (i.e. sum of the root densities at the 40 x 50 cm plot is 100%). This means that if the root density in one segment is changed, then the root densities of all segments would be changed as well. Thus, density values obtained from different techniques actually cannot closely correspond. Different root density patterns could be attributed to the fact that fine roots of high density (visible on the image, Figure 1) could have lower weights in comparison to the weight of few large roots. This is most apparent when comparing results for barley (Figures 1a, b, 2, 4a and 5). Higher root densities were obtained at the depths 30 to 45 cm using the image analyses in comparison to those resulting from gravimetric analysis. The ratios between root densities (Figure 4a) from image and gravimetric analysis are 1.38 for barley in the single row and the depth of 32.5 cm, and 1.14, 1.41 and 1.31 for barley rows cross section and the depths 32.5, 37.5 and 42.5 cm, respectively. Conversely, slightly lower root densities were obtained at the upper part using image analyses in comparison to those resulting from gravimetric analysis. For instance, the ratios between root densities (Figure 4a) from image and gravimetric analysis are 0.70 and 0.71 for barley in the single row and the depth of 17.5 and 22.5 cm, respectively, and 0.75, 0.70 and 0.75 for barley rows cross section and the depths 2.5, 7.5 and 12.5 cm, respectively. Many fine roots extract water more effectively from soil than few large roots, which associates not only with their length (e.g. Bingham and Wu, 2011; Chen et al., 2014; Himmelbauer and Novák, 2008; Lü et al., 2015; Zhang et al. 2015) and surface (Himmelbauer et al., 2004, 2013), but also on their physiology (Sinha, 2004) and ability to interact closely with the soil material (Hillel, 2004).

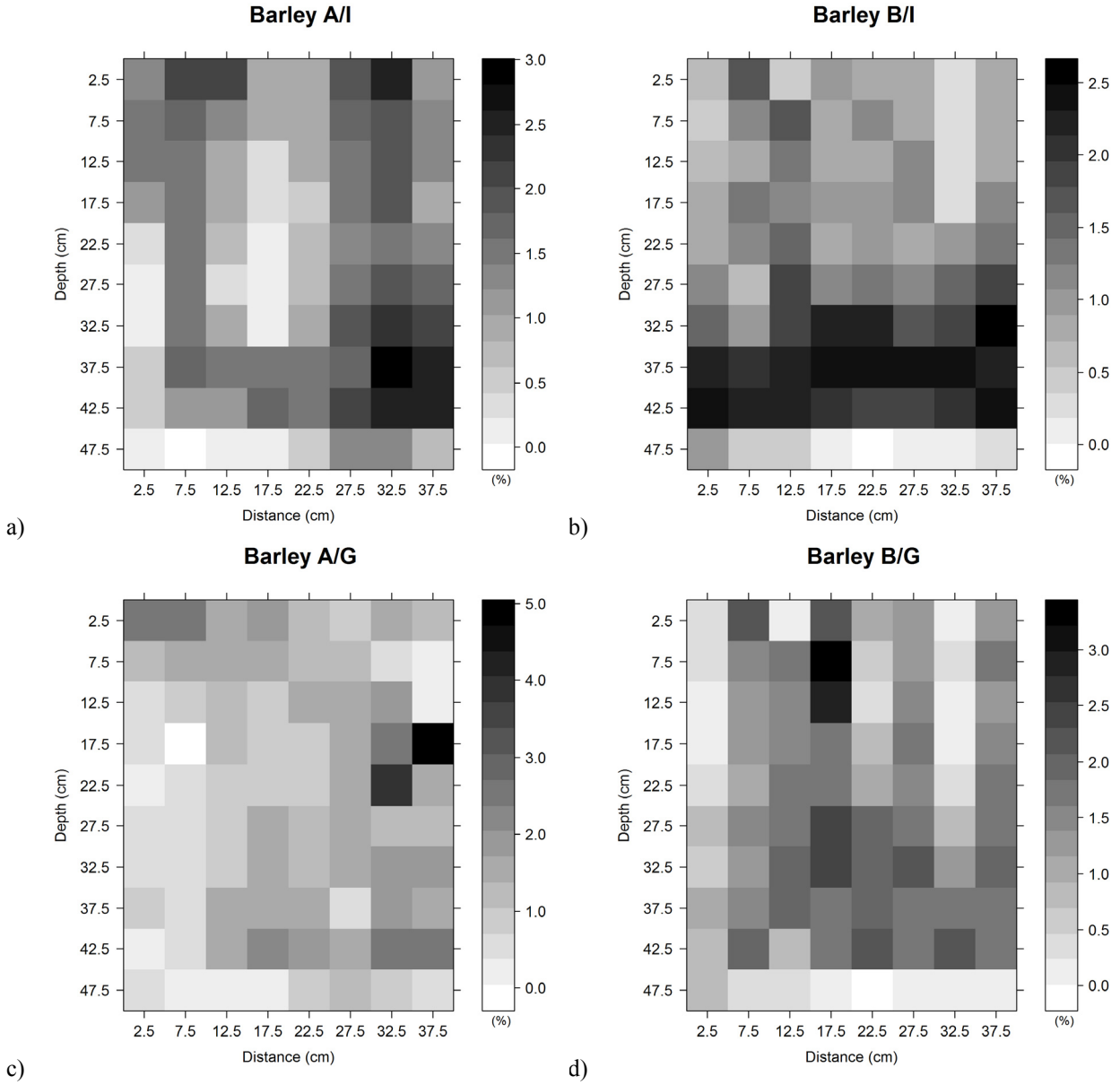

Fig. 2. Areal barley root densities in row (A) and rows cross section (B) evaluated using image (I) and gravimetric (G) analysis.

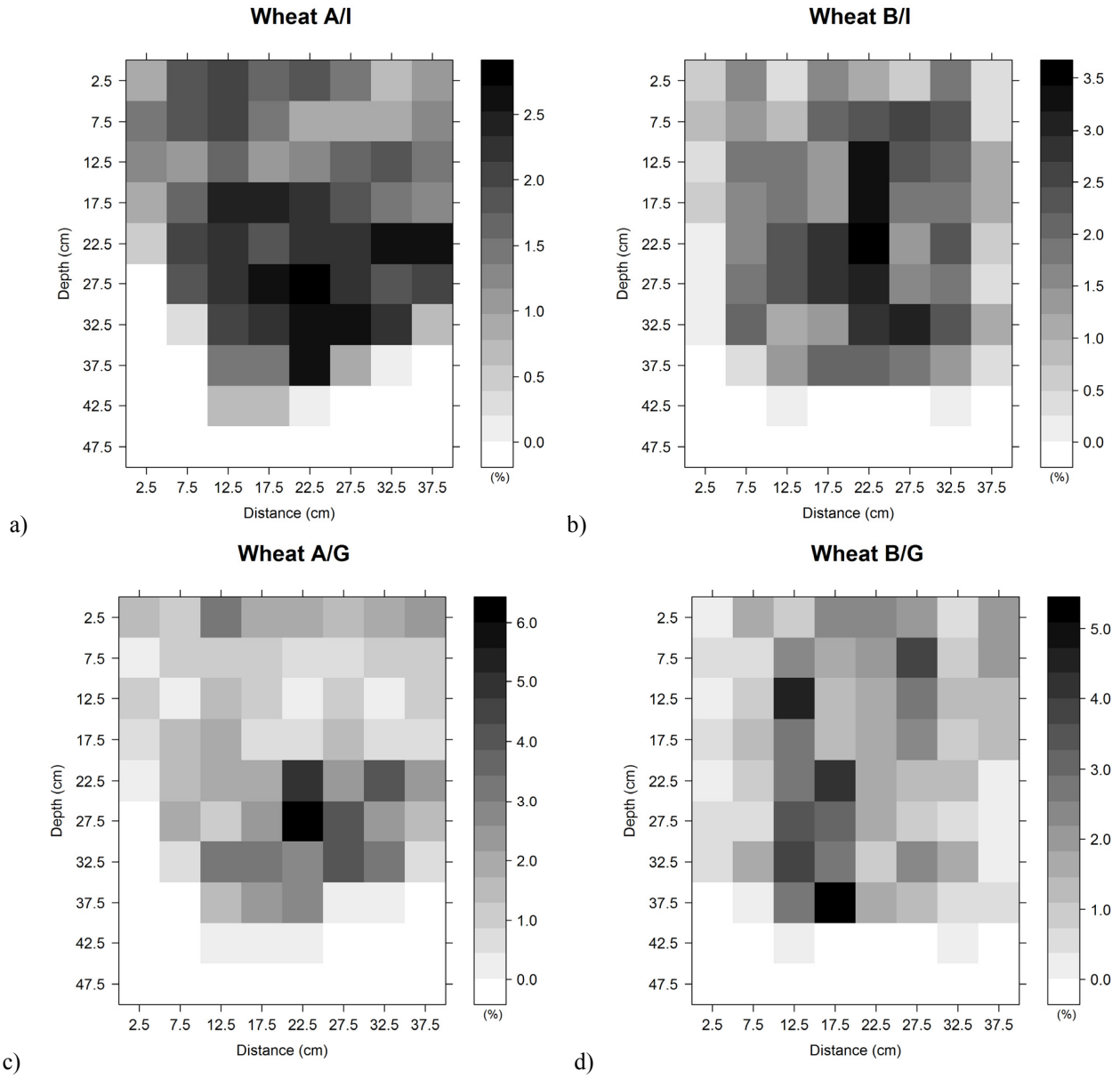

Fig. 3. Areal wheat root densities in row (A) and rows cross section (B) evaluated using image (I) and gravimetric (G) analysis.

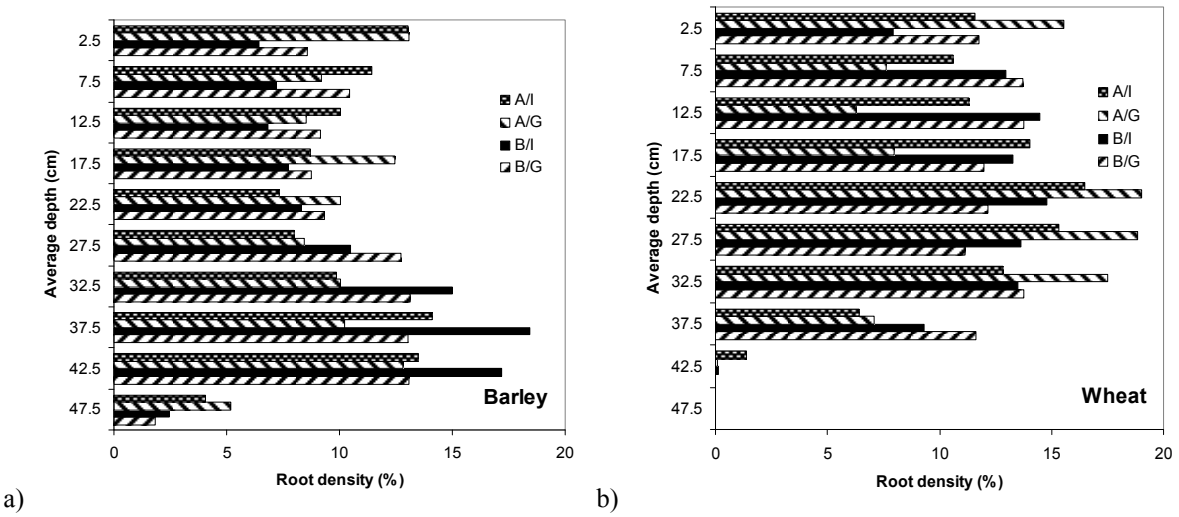

Fig. 4. Vertical root densities in rows (A) and rows cross sections (B) obtained using image (I) or gravimetric (G) analysis.

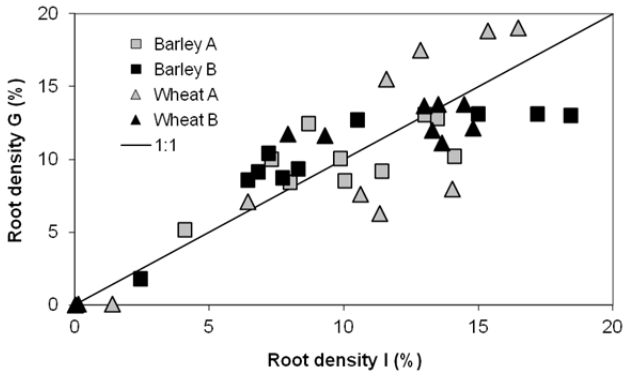

Fig. 5. Relationship between vertical root densities (A - rows, B - rows cross sections) evaluated using both techniques, i.e. image (I) and gravimetric (G) analysis.

Therefore, in such cases the image technique provides more reliable data than the gravimetric method. On the other hand, in many segments roots overlapped each other and therefore were not visible on the image (Figure 1). This is most visible at the bottom part (depth of 20 to 35 cm) of the root zone of wheat sown in the single row (Figure 1c, d, 3, 4b and 5), where roots formed dense clusters. Thus lower root densities (with respect to the entire root zone) were obtained in comparison to that from the gravimetric analysis. The ratios between root densities (Figure 4b) from image and gravimetric analysis are 0.87, 0.81 and 0.73 for wheat in the single row and the depth of 22.5, 27.5 and 32.5 cm, respectively. In this case, the proposed image technique provided less reliable data than the gravimetric method. However, a part of this problem may be overcome, if a program like WinRhizo (Arsenault et al., 1995) would be used to detect overlapping roots. For instance, Himmelbauer et al. (2004) applied this program to evaluate root length, diameter and area and to compare result with parameters obtained using ROOTEDGE (Kaspar and Ewing, 1997). However, they obtained similar results, because they did not scan root clusters. Another possibility would be to apply algorithm for root reconstruction. For instance Stingaciu et al. (2013) applied an automatic algorithm described by Schulz et al. (2012). However, they used three-dimensional MRI images. A thinner root zone layer may also be analyzed. Our box thickness was the same as in the study by Moradi et al. (2010). Thinner boxes were used for example by Whiting et al. (2000) 2 cm, Rudolph et al. (2012) 0.5 cm, and Youssef and Chino (1988) 1 mm. However, such a narrow space for root growth strongly affects the root architecture. It should be also noted that wheat roots usually do not form such dense clusters (e.g. Chen et al., 2014) as were formed in our laboratory box.

Descriptive statistics of all evaluated root densities are shown in Tables 2, 3, 4 and 5. The same averages (Tables 2 and 4) were obtained for all A, B, I and G combinations when using all data, or when removing only zero values, because the sum of all root densities within the 1D or 2D mesh is always 100%. Larger averages (Table 3 and 5) were calculated when mesh rows with zero and very low values were removed from all data sets. Standard deviations, coefficients of variations and ranges (maximum – minimum) (Table 2 and 3) indicate that the areal root densities resulting from the gravimetric analysis were in all cases more variable (i.e. had higher deviation from the mean) than root densities obtained using the image analysis. However the opposite trend (except for wheat sown in the single row) was observed when comparing standard deviations, coefficients of variations and ranges for vertical root densities. The reason is that the sum of values in each layer eliminated the impact of the horizontal variability, which was larger for data obtained from the gravimetric analysis than that from the image analysis (Figures 2 and 3). Correlation coefficients relating root densities resulting from different techniques are shown in Table 6, 7 and 8. The lower R values were mostly obtained when excluding lines with zero and low values. Correlation coefficients for areal root densities (Table 6) show relatively poor and moderate correlations between root densities obtained using different techniques, despite that the statistical significance of the estimated correlations was at the 99.0% confidence level and larger. Larger R values (Tables 7 and 8) were obtained when relating vertical root densities from different techniques, but the statistical significance of the estimated correlations was lower. The reason is that the RDS values were more variable than RDD data (i.e. range of RDS values was higher than range of RDD values). Again, the R values and statistical significance decrease after removing very low values.

Table 2. Basic statistics of areal root density (%).

	Barley A/I	Barley A/G	Barley B/I	Barley B/G	Wheat A/I	Wheat A/G	Wheat B/I	Wheat B/G
Count	80	80	80	80	80	80	80	80
Average	1.25	1.25	1.25	1.25	1.25	1.25	1.25	1.25
Standard deviation	0.689	0.797	0.699	0.747	0.910	1.276	1.014	1.204
Coeff. of variation (%)	55.12	63.72	55.90	59.78	72.80	102.08	81.09	96.30
Minimum	0.02	0.029	0.0	0.0	0.0	0.0	0.0	0.0
Maximum	2.81	4.724	2.49	3.219	2.72	6.01	3.43	5.094

Table 3. Basic statistics of areal root density (%) after removing zero and very low values (values at depths of 45–50 and 35–50 cm for barley and wheat, respectively).

	Barley A/I	Barley A/G	Barley B/I	Barley B/G	Wheat A/I	Wheat A/G	Wheat B/I	Wheat B/G
Count	76	76	76	76	59	59	59	59
Average	1.27	1.27	1.31	1.31	1.67	1.69	1.68	1.66
Standard deviation	0.699	0.813	0.666	0.715	0.653	1.207	0.828	1.140
Coeff. of variation (%)	55.23	64.21	50.89	54.47	39.03	71.27	49.33	68.58
Minimum	0.02	0.029	0.13	0.063	0.11	0.128	0.06	0.076
Maximum	2.81	4.724	2.49	3.219	2.72	6.007	3.43	5.094

Table 4. Basic statistics of vertical root densities (%) (zero values at the depths 45–50 cm for wheat were removed).

	Barley A/I	Barley A/G	Barley B/I	Barley B/G	Wheat A/I	Wheat A/G	Wheat B/I	Wheat B/G
Count	10	10	10	10	9	9	9	9
Average	10.0	10.0	10.0	10.0	11.11	11.11	11.11	11.11
Standard deviation	3.13	2.41	5.20	3.46	4.68	6.76	4.73	4.27
Coeff. of variation (%)	31.30	24.07	52.03	34.63	42.13	60.81	42.60	38.40
Minimum	4.07	5.16	2.44	1.81	1.38	0.09	0.13	0.06
Maximum	14.11	13.1	18.42	13.13	16.48	19.02	14.79	13.78

Table 5. Basic statistics of vertical root densities (%) (after removing low values at depths of 45–50 cm and 40–450 cm for barley and wheat, respectively).

	Barley A/I	Barley A/G	Barley B/I	Barley B/G	Wheat A/I	Wheat A/G	Wheat B/I	Wheat B/G
Count	9	9	9	9	8	8	8	8
Average	10.66	10.54	10.84	10.91	12.33	12.49	12.49	12.49
Standard deviation	2.48	1.81	4.75	2.04	3.13	5.71	2.50	1.08
Coeff. of variation (%)	23.25	17.15	43.78	18.73	25.43	45.75	19.99	8.68
Minimum	7.32	8.45	6.42	8.57	6.43	6.3	7.91	11.13
Maximum	14.11	13.1	18.42	13.13	16.48	19.02	14.79	13.78

Table 6. Pearson correlation coefficient (from the regression analysis using Statgraphics, 2009) exposing relationships between evaluated areal root densities.

	Barley		Wheat	
Count	80 [a]	76 [b]	80 [a]	59 [b]
A/I and A/G	0.429*** [a]	0.422*** [b]	0.778*** [a]	0.643*** [b]
B/I and B/G	0.579*** [a]	0.514*** [b]	0.624*** [a]	0.369** [b]

[a] all data, [b] data after removing zero and very low values, * $p < 0.05$, ** $p < 0.01$, *** $p < 0.001$.

Table 7. Pearson correlation coefficient (from the regression analysis using Statgraphics, 2009) exposing relationships between evaluated vertical root densities (%) for barley.

	Barley A/I	Barley A/G	Barley B/I	Barley B/G
Barley A/I	1	0.698* [a]	0.652* [a]	–
Barley A/G	0.430 [b]	1	–	0.511 [a]
Barley B/I	0.486 [b]	–	1	0.846** [a]
Barley B/G	–	–0.194 [b]	0.883** [b]	1

[a] all data, [b] data after removing low values, * $p < 0.05$, ** $p < 0.01$, *** $p < 0.001$.

Table 8. Pearson correlation coefficient (from the regression analysis using Statgraphics, 2009) exposing relationships between evaluated vertical root densities (%) for wheat.

	Wheat A/I	Wheat A/G	Wheat B/I	Wheat B/G
Wheat A/I	1	0.814** [a]	0.872** [a]	–
Wheat A/G	0.680 [b]	1	–	0.536 [a]
Wheat B/I	0.627 [b]	–	1	0.893** [a]
Wheat B/G	–	–0.308 [b]	0.411 [b]	1

[a] all data, [b] data after removing low values, * $p < 0.05$, ** $p < 0.01$, *** $p < 0.001$.

Comparison of root distributions of plants sown in single row and in selected spots (i.e. simulated rows cross section)

Vertical root densities (Figure 4) and correlation coefficients relating vertical root densities obtained using a particular technique (i.e. either image or gravimetric analysis) from A and B sowing scenarios for each cereal (Tables 7 and 8) show significant positive relationships between values obtained using the image analysis for both cereals and assuming all depths (i.e. all values). This would indicate that both sowing scenarios resulted in similar vertical root distributions. However, relationships between data sets after removing low values were not significant. The R and p values calculated for data obtained from the gravimetric analysis showed insignificant positive relationships between root densities when analyzing all values, and insignificant negative relationships when excluding low values.

In studies published for instance by Bingham and Wu (2011), Chen et al. (2014), Himmelbauer and Novák (2008), Lü et al. (2015) or Zhang et al. (2015), the largest barley or wheat root densities (that were evaluated mostly under field conditions) were usually observed at the top of the soil profile and decreased exponentially with depth. In our case (Figure 4), larger root densities of barley root were obtained at the bottom part of the laboratory box (i.e. at the depths 30 to 45 cm) than at its upper part, and relative homogeneous root distribution with depth was obtained for wheat. This may be attributed to our laboratory conditions, i.e. substrate layer thickness of only 50 cm restricting root grow (in the case of barley) and larger soil water contents at the bottom of the sandy substrate stimulating root growth to greater depth. The shallow roots of wheat, and dieback of both crops at particular stages, also indicate unfavorable conditions for plant development (i.e. limited space in the box, not suitable soil water and nutrient conditions in substrate, relatively stable temperature and humidity in the greenhouse, etc.).

Comparison of simulated root water uptakes using different vertical root distributions

Simulated root water uptakes for both cereals and all scenarios (i.e. root densities resulted from two sowing types and two analytical methods) are shown in Figure 6. At the beginning, all simulated root water uptakes followed potential root water uptake. Figure 6a shows that both scenarios with the root densities for barley sown in a single row (A) reached the limit of decreased water availability sooner (root water uptake earlier started decreasing) than the scenarios for seeds sown in several spots (B). The reason is that the higher root densities (Figure 4a) were set at the upper parts of initial lower water content and

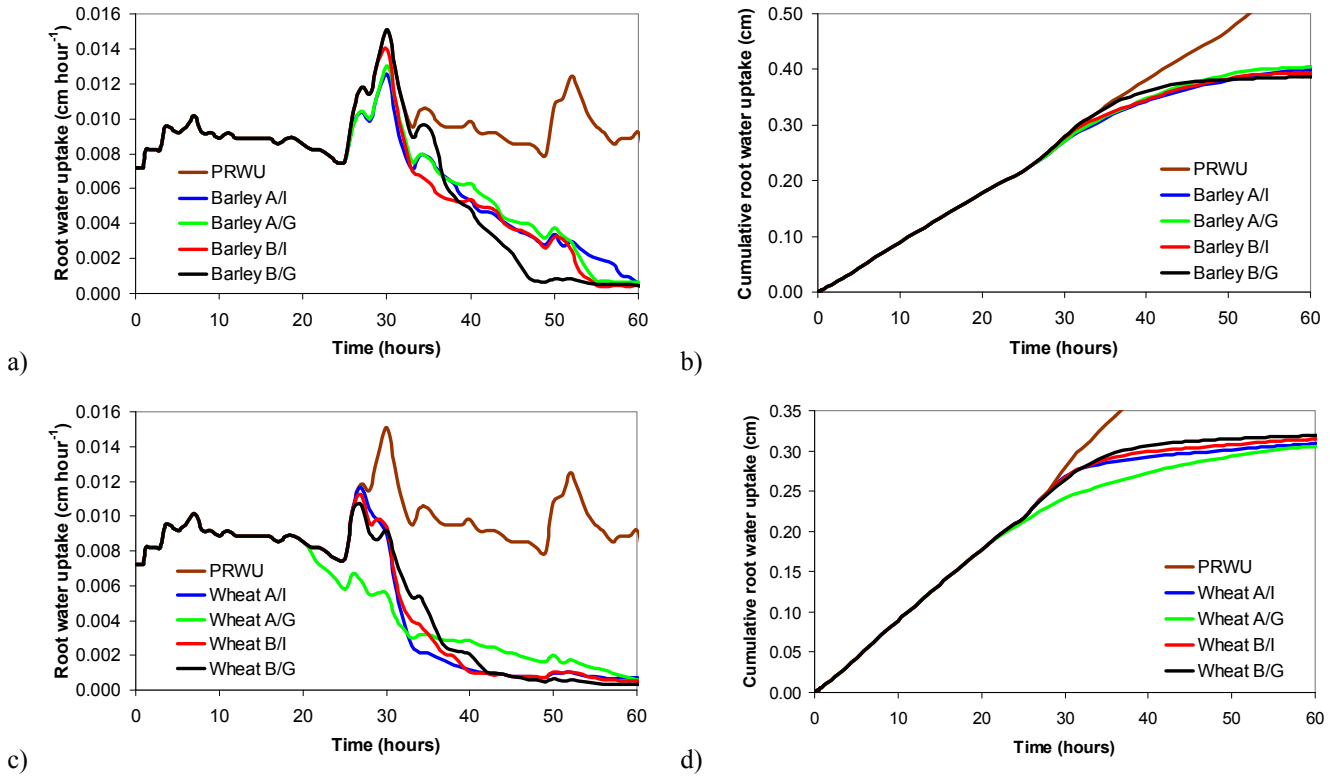

Fig. 6. Root water uptakes and cumulative root water uptakes simulated using HYDRUS-1D for barley (a and b, respectively) and wheat (c and d respectively): PRWU - potential root water uptake, A – row, B – rows cross section, I - root density from image analysis, G - root density from gravimetric analysis.

lower root densities at the bottom part of initially higher water content (i.e. lower initial pressure head of –155 cm at the top in comparison to pressure head of = –100 cm at the bottom of the substrate) in the case of A scenarios. The lower root densities (Figure 4a) were set at the upper parts of initial lower water content and higher root densities at the bottom part of initially higher water content for B scenarios. Since water fluxes within the flow domain were negligible (due to steady state conditions at the beginning and low hydraulic conductivities corresponding to low simulated pressure heads), setting larger root densities (i.e. larger values of normalized water uptake) at the depths of larger initial water storage insured water availability for a longer time in comparison to scenarios when setting larger root densities at the depths of lower initial water storage. On the other hand, the root water uptake decline for A scenarios was not as steep as that for B scenarios, due to the fact that greater root densities were at the bottom part (i.e. the part of higher pressure heads and soil water content). When comparing scenarios with root densities resulting from different techniques, it is evident that a larger difference was obtained for B scenarios. The B/I scenario shows an earlier but more gradual root water uptake decline than that from the B/G scenario (Figure 6a). The reason is that while B/G root densities increased only slightly with increasing depth (i.e. followed increasing water contents), the B/I root densities set at the bottom part (depths of 30–45 cm) were approximately twice higher in comparison to those at the top part (Figure 4a). Therefore, root water uptake at the bottom part was reduced. The simulated wheat root water uptakes (Figure 6c) started to diverge from potential values sooner than those for barley (Figure 6a), due to a lower root zone depth (i.e. due to lower water storage available for root water uptake). Simulated root water uptake from wheat A/G scenario greatly differs from those for the other 3 wheat scenarios (Figure 6c). In this case the reason is that the roots overlapped each other and therefore were not visible on the image. As a result, lower root densities were obtained in comparison to those from the gravimetric analysis (Figure 4b). While wheat A/I root densities increased only slightly with increasing depth (i.e. followed increasing water contents), the A/G root densities at the depths of 20–35 cm were approximately two times higher in comparison to those at the depth of 5–20 cm. Therefore in the case of A/G scenario, the root water uptake at the lower part was (due to a decreased water availability) reduced sooner than in the case of A/I scenario (i.e. the root water uptake for A/G scenario declined sooner but more gradually in comparison to that for A/I scenario).

Despite the fact that simulated actual root water uptakes varied, all scenarios for a particular cereal reached the same cumulative root water uptakes at the end (Figures 6b and 6d). The reason was that the same root zone depth was set for each cereal and water storage within the flow domain was not influenced by water fluxes across the top and bottom boundaries.

Comparison of simulated root water uptakes using vertical and areal root distributions

Figure 7 shows root water uptake for scenario A/I simulated using HYDRUS-1D (also presented in Figure 6) and HYDRUS-2D, which were similar regardless of the fact that the water content distributions (Figures 8 and 9) showed slightly different trends (e.g. remaining water and not remaining water at the end of the simulations in the middle of 2D and 1D flow domain, respectively,). It can be assumed that the impact of the horizontal root density distribution was less important than

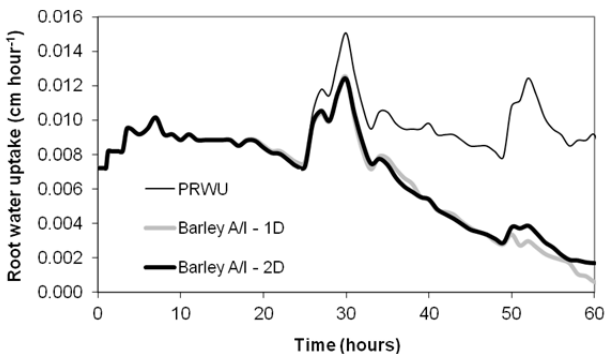

Fig. 7. Barley root water uptakes simulated using HYDRUS-1D and HYDRUS-2D: PRWU - potential root water uptake, A – row, I - root density from image analysis.

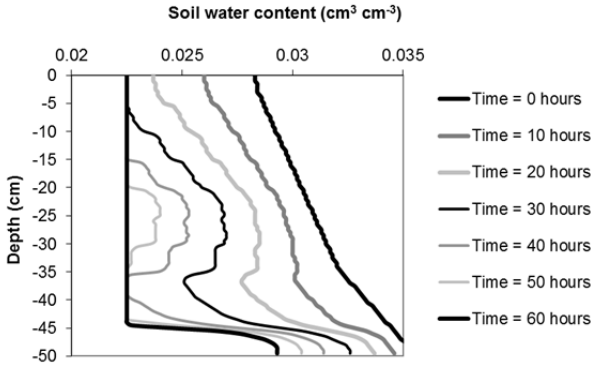

Fig. 8. Water contents in sand-vermiculite substrate simulated using HYDRUS-1D for barley in row and root density evaluated using image analysis.

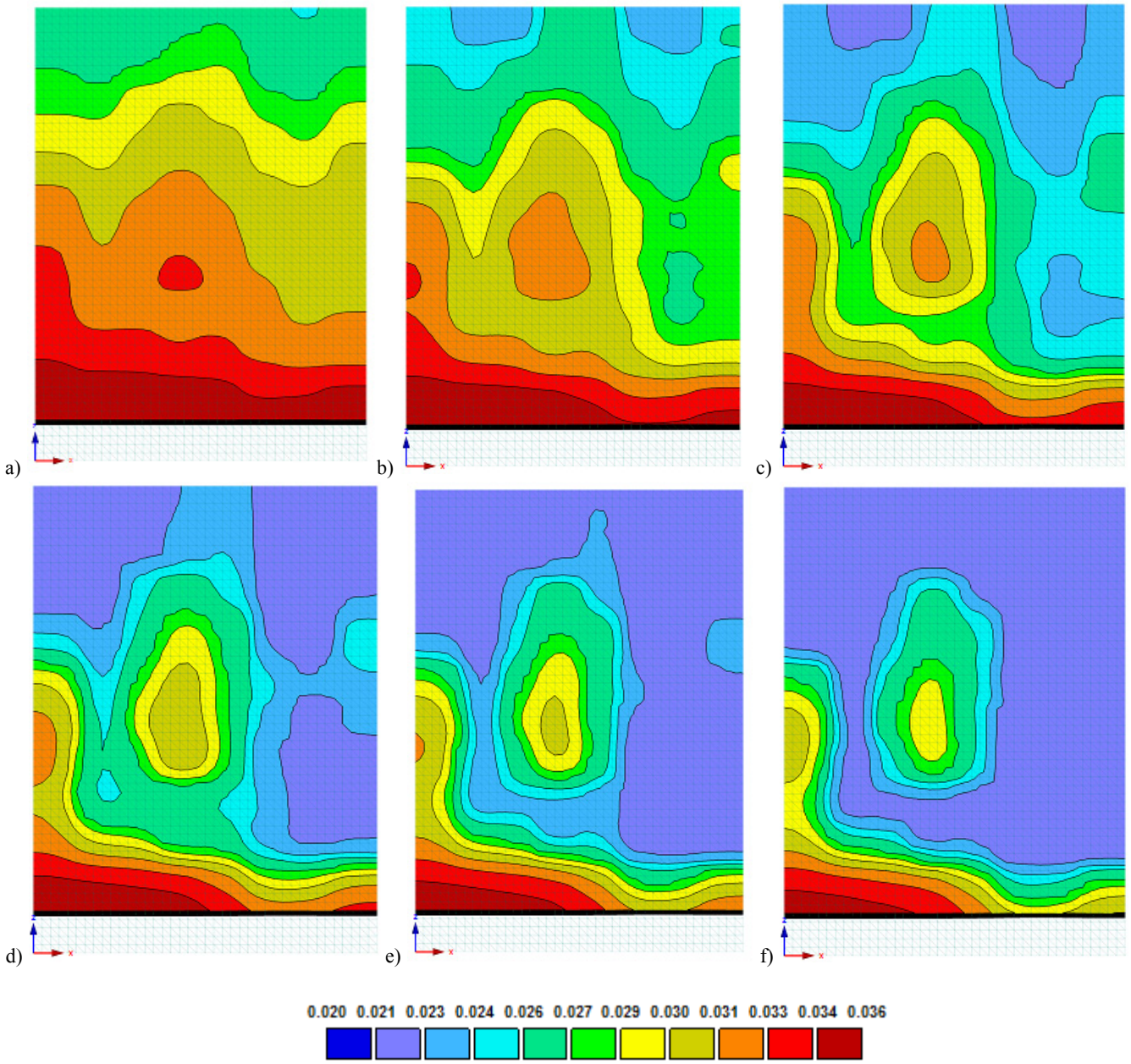

Fig. 9. Water contents (cm^3 cm^{-3}) in sand-vermiculite substrate simulated using HYDRUS-2D for barley in row and root density evaluated using image analysis 10 (a), 20 (b), 30 (c), 40 (d), 50 (e) and 60 (f) hours from the simulation beginning.

the impact of the vertical root distribution due to the initial hydrostatic water distribution in the soil profile (i.e. water content did not initially vary along horizontal axes and water fluxes were negligible). It should be noted that differences between the results of 2D and 1D scenarios and also differences between 1D scenarios with variable vertical root distribution would be probably smaller, if the compensated root water uptake (Šimůnek and Hopmans, 2009) is considered (i.e. decreased root water uptake at regions of low pressure heads would be compensated from zones of higher pressure heads).

The water compensation would depend on the critical stress index (in such case smaller than one) in the root water uptake model. On the other hand, the simulated 2D soil water content pattern (Figure 9) corresponds to a visually observed water distribution in the sand-vermiculite substrate (i.e. lower water content at zones with higher root density and opposite). Thus, we suggest that scenarios (which neglected water compensation) relatively well approximated conditions in our laboratory box (which were given by the box design, substrate texture and corresponding soil hydraulic properties, and root texture). We assume that water compensation would play a greater role under natural conditions (i.e. real soil material, deeper and more diverse root system and natural soil water regime). It should also be noted that our 2D scenario did not allow a description of soil water contents within the flow domain in such detail as in the study by Doussan et al. (2006), who simulate soil water extraction using the hydraulic tree model of root system (i.e. by assuming real root system architecture, root water flow, hydraulic pumping etc.). However, for practical purposes, a more simple description of soil-roots interaction seems to be more useful.

CONCLUSIONS

Barley and wheat root distributions were studied in a flat laboratory box. The application of two techniques (image processing and gravimetric) for root density analysis resulted into noticeably different root density distributions. The main reasons were: 1) fine roots of high density (located mostly at the bottom part of the box) had lower weights in comparison to weight of few large roots (situated at the upper part of the box); 2) in contrast, roots overlapped each other and were not visible on the image. In some cases roots even formed dense clusters (which were mostly developed in the wheat root zone), and root density from image analysis was underestimated. Since fine roots mainly participate in water uptake, we can conclude that image analysis more reliably described barley root densities in comparison to those assessed using gravimetric analysis. On the other hand, less reliable data were obtained using image processing compared to those evaluated using the gravimetric method for wheat. However, in this case, artificial box conditions greatly affected root growth, which resulted in atypical root system architecture.

Different root densities obtained using two techniques resulted in diverse root water uptakes, as simulated using HYDRUS-1D. Initially the same simulated actual root water uptakes (which followed potential root water uptake) started to decline from potential values depending on actual water content at the depth of the highest root density. Usually, an earlier downtrend associates with gradual root water uptake decreas and vice versa. Similar root water uptakes were simulated using the HYDRUS-1D and HYDRUS-2D models for the selected scenario (i.e. root density for barley sown in a single row evaluated using the image analysis). The impact of the horizontal root density distribution on root water uptake was, in this case, less important than the impact of the vertical root distribution resulting from different techniques and sowing scenarios.

In conclusion, our study showed that root densities, which are then used in HYDRUS-1D and 2D for simulating soil water regime and root water uptake, can be obtained by image analysis using standard image processing programs. The proposed method (using an image analysis of the entire root system) should be further validated using a deeper laboratory box (to avoid root growth restriction) and via performing additional analyses that allow the application of programs usually used for describing root parameters (e.g. root length, diameter, surface area). Programs like WinRhizo can be utilized not only to obtain additional information about roots, but also for correcting results from simple image analysis (i.e. reconstructing overlapping roots). Water regime (e.g. fluxes at the top and bottom boundary, actual root uptake, water contents within the box, etc.) should be also monitored to be compared with simulated data to reveal the degree of accuracy for root density description, which is necessary for reliable description of soil water regime with mathematical models.

Acknowledgement. Authors acknowledge the financial support of the Czech Science Foundation (No. 13-12477S) and the Ministry of Agriculture of the Czech Republic (QJ1230319). Authors also thank Christopher Ash for English language correction.

REFERENCES

Arsenault, J.L., Pouleur, S., Messier, C., Guay, R., 1995. WinRHIZO, a root-measuring system with a unique overlap correction method. HortScience, 30, 906.

Bengough, A.G., McKenzie, B.M., Hallett, P.D., Valentine, T.A., 2011. Root elongation, water stress, and mechanical impedance: a review of limiting stresses and beneficial root tip traits. Journal of Experimental Botany, 62, 1, 59–68.

Bingham, I.J., Wu, L., 2011. Simulation of wheat growth using the 3D root architecture model SPACSYS: Validation and sensitivity analysis. European Journal of Agronomy, 34, 181–189.

Chen, Y.L., Palta, J., Clements, J., Buirchelld, B., Siddiqueb, K.H.M., Rengel, Z., 2014. Root architecture alteration of narrow-leafed lupin and wheat in response to soil compaction. Field Crops Research, 165, 61–70.

Dane, J.H., Topp, G.C., 2002. Methods of Soil Analysis, Part 4, Physical Methods. SSSA, Madison, USA, 1692 p. ISBN: 0-89118-841-X

de Dorlodot, S., Forster, B., Pages, L., Price, A., Tuberosa, R., Draye, X., 2007. Root system architecture: opportunities and constraints for genetic improvement of crops. Trends in Plant Science, 12, 10, 474–481.

Doussan, C., Pierret, A., Garrigues, E., Pagès, L., 2006. Water uptake by plant roots: II – Modelling of water transfer in the soil root-system with explicit account of flow within the root system – Comparison with experiments. Plant and Soil, 283, 1–2, 99–117.

Feddes, R.A., Kowalik, P.J., Zaradny, H., 1978. Simulation of Field Water Use and Crop Yield. John Wiley, New York, 188 p.

Garrigues, E., Doussan, C., Pierret A., 2006. Water uptake by plant roots: I – Formation and Propagation of a Water Extraction Front in Mature Root Systems as Evidenced by

2D Light Transmission Imaging. Plant and Soil, 283, 1–2, 83–98.

Hallett, P.D., Karim, K.H., Bengough, A.G., Otten, W., 2013. Biophysics of the vadose zone: From reality to model systems and back again. Vadose Zone Journal, 12, 4, DOI: 10.2136/vzj2013.05.0090

Hillel, D., 2004. Introduction to Environmental Soil Physics. Elsevier Academic Press, Amsterdam. ISBN 0-12-348655-6.

Himmelbauer, M.L., Novák, V., 2008. Root distribution functions of spring barley, winter rye and maize. Die Bodenkultur, 59, 1–4, 165–172.

Himmelbauer, M.L., Loiskandl, W., Kastanek, F., 2004. Estimating length, average diameter and surface area of roots using two different Image analyses system. Plant and Soil, 260, 1–2, 111–120.

Himmelbauer, M.L., Loiskandl, W., Rousseva, S., 2010. Spatial root distribution and water uptake of maize grown on field with subsoil compaction. Journal of Hydrology and Hydromechanics, 58, 3, 163–174.

Himmelbauer, M.L., Vateva, V., Lozanova, L., Loiskandl, W., Rousseva, S., 2013. Site effects on root characteristics and soil protection capability of two cover crops grown in South Bulgaria. Journal of Hydrology and Hydromechanics, 61, 1, 30–38.

Iversen, C.M., Murphy, M.T., Allen, M.F., Childs, J., Eissenstat, D.M., Lilleskov, E.A., Sarjala, T.M., Sloan, V.L., Sullivan, P.F., 2012. Advancing the use of minirhizotrons in wetlands. Plant and Soil, 352, 1–2, 23–39.

Kaspar, T.C., Ewing, R.P., 1997. ROOTEDGE: Software for Measuring Root Length from Desktop Scanner Images. Agronomy Journal, 89, 6, 932–940.

Kodešová, R., Kodeš, V., Žigová, A., Šimůnek, J., 2006. Impact of plant roots and soil organisms on soil micromorphology and hydraulic properties. Biologia, 61(Suppl. 19), S339–S343.

Kodešová, R., Němeček, K., Žigová, A., Nikodem, A., Fér, M., 2015. Using dye tracer for visualizing roots impact on soil structure and soil porous system. Biologia, 70, 11, 1439–1443.

Loades, K.W., Bengough, A.G., Bransby, M.F., Hallett, P.D., 2013. Biomechanics of nodal, seminal and lateral roots of barley: effects of diameter, waterlogging and mechanical impedance. Plant and Soil, 370, 1–2, 407–418.

Lü, G.H., Song, J.Q., Bai, W.B., Wu, Y.F., Liu, Y., Kang, Y. H., 2015. Effects of different irrigation methods on microenvironments and root distribution in winter wheat fields. Journal of Integrative Agriculture, 14, 8, 1658–1672.

Maeght, J.L., Rewald, B., Pierret, A., 2013. How to study deep roots–and why it matters. Frontiers in Plant Science. 4, Article 299.

Moradi, A.B., Conesa, H.M., Robinson, B., Lehmann, E., Kuehne, G., Kaestner, A., Oswald, S., Schulin, R., 2009. Neutron radiography as a tool for revealing root development in soil: capabilities and limitations. Plant and Soil, 318, 1–2, 243–255.

Moradi, A.B., Oswald, S.E., Nordmeyer-Massner, J.A., Pruessmann, K.P., Robinson, B.H., Schulin, R., 2010. Analysis of nickel concentration profiles around the roots of the hyperaccumulator plant Berkheya coddii using MRI and numerical simulations. Plant and Soil, 328, 1, 291–302.

Moradi, A.B., Hopmans, J.W., Oswald, S.E., Menon, M., Carminati, A., Lehmann, E., 2013. Applications of Neutron Imaging in Soil–Water–Root Systems. In: Anderson, S.A., Hopmans, J.W. (Eds.): Soil–Water–Root Processes: Advances in Tomography and Imaging. American Society of Agronomy, Soil Science Society of America, Crop Science Society of America, Madison, USA, pp. 113–136. ISBN: 978-0-89118-959-6.

Moran, C.J., Pierret, A., Stevenson, A.W., 2000. X-ray absorption and phase contrast imaging to study the interplay between plant roots and soil structure. Plant and Soil, 223, 1–2, 99–115.

Neumann, G., George, T.S., Plassard, C., 2009. Strategies and methods for studying the rhizosphere–the plant science toolbox. Plant and Soil, 321, 1–2, 431–456.

Nikodem, A., Pavlů, L., Kodešová, R., Borůvka, L., Drábek, O., 2013. Study of podzolization process under different vegetation cover in the Jizerské hory Mts. region. Soil and Water Research, 8, 1, 1–12.

Novák, V., 2012. Evapotranspiration in the Soil-Plant-Atmosphere System. Springer, Dordrecht, 253 p.

Oswald, S.E., Menon, M., Carminati, A., Vontobel, P., Lehmann, E., Schulin, R., 2008. Quantitative imaging of infiltration, root growth, and root water uptake via neutron radiography. Vadose Zone Journal, 7, 3, 1035–1047.

Rasband, W.S., 1997–2014. ImageJ, U. S. National Institutes of Health, Bethesda, Maryland, USA, http://imagej.nih.gov/ij/.

Rudolph, N., Esser, H.G., Carminati, A., Moradi, A.B., Hilger, A., Kardjilov, N., Nagl, S., Oswald, S.E., 2012. Dynamic oxygen mapping in the root zone by fluorescence dye imaging combined with neutron radiography. Journal of Soils and Sediments, 12, 1, 63–74.

Rudolph, N., Voss, S., Moradi, A.B., Nagl, S., Oswald, S.E., 2013. Spatio-temporal mapping of local soil pH changes induced by roots of lupin and soft-rush. Plant and Soil, 369, 1–2, 669–680.

Rudolph-Mohr, N., Vontobel, P., Oswald, S.E., 2014. A multi-imaging approach to study the root–soil interface. Annals of Botany, 114, 8, 1779–1787.

Schulz, H., Postma, A.J., van Dusschoten, D., Scharr, H., Behnke, S., 2012. 3D reconstruction of plant roots from MRI images. In: Csurka, G., Braz, J. (Eds.): Proceedings of the International Conference on Computer Vision Theory and Applications, VISAPP 2012, Rome, 24–26 February 2012.

Shilo, T., Rubin, B., Ephrath, J.E., Eizenberg, H., 2013. Continuous non-destructive monitoring of *Cyperus rotundus* development using a minirhizotron. Weed Research, 53, 3, 164–168.

Šimůnek, J., van Genuchten M.T., Šejna, M., 2008. Developmental and applications of the HYDRUS and STANMOD Software Packages and Related Codes. Vadose Zone Journal, 7, 587–600.

Šimůnek, J., Hopmans, J.W., 2009. Modeling compensated root water and nutrient uptake, Ecological Modeling, 220, 4, 505–521.

Sinha, R.K. 2004. Modern plant physiology. Alpha Science International, Pangbourne, 635 p. ISBN 1-84265-029-7.

Stingaciu, L., Schulz, H., Pohlmeier, A., Behnke, S., Zilken, H., Javaux, M., Vereecken, H., 2013. In situ root system architecture extraction from magnetic resonance imaging for water uptake modeling. Vadose Zone Journal, 12, 1. DOI: 10.2136/vzj2012.0019.

Tron, S., Bodner, G., Laio, F., Ridolfi, L., Leitner, D., 2015. Can diversity in root architecture explain plant water use efficiency? A modeling study. Ecological Modelling, 312, 200–210.

van Dam, J.C., Stricker, J.M.N., Droogers, P., 1994. Inverse method to determine soil hydraulic function from multi-step

outflow experiment. Soil Science Society of America Journal, 58, 3, 647–652.

van Genuchten, M.Th., 1980. A closed-form equation for predicting the hydraulic conductivity of unsaturated soils. Soil Science Society of America Journal, 44, 5, 892–898.

Whiting, S.N., Leake, J.R., McGrath, S.P., Baker, A.J.M., 2000. Positive responses to Zn and Cd by roots of the Zn and Cd hyperaccumulator Thlaspi caerulescens. New Phytologist, 145, 199–210.

Youssef, R.A., Chino, M., 1988. Development of a new rhizobox system to study the nutrient status in the rhizosphere, Soil Science and Plant Nutrition, 34, 3, 461–465, DOI: 10.1080/00380768.1988.10415701.

Zhang, X., Zhang, X., Liu, X., Shao, L., Sun, H., Chen, S., 2015. Incorporating root distribution factor to evaluate soil water status for winter wheat. Agricultural Water Management, 153, 32–41.

Received 10 August 2015
Accepted 16 December 2015